

FAST TRACK COMMUNICATION

Direct and core-resonant double photoemission from Cu(001)

Grant van Riessen, Zheng Wei, Rajendra S Dhaka,
Carsten Winkler, Frank O Schumann and Jürgen Kirschner

Max-Planck-Institut für Mikrostrukturphysik, Weinberg 2, D-06120 Halle, Germany

Received 27 January 2010, in final form 29 January 2010

Published 15 February 2010

Online at stacks.iop.org/JPhysCM/22/092201

Abstract

We have measured the correlated electron pair emission from a Cu(001) surface by both direct and core-resonant channels upon excitation with linearly polarized photons of energy far above the 3p threshold. As expected for a single-step process mediated by electron correlation in the initial and final states, the two electrons emitted by the direct channel continuously share the sum of the energy available to them. The core-resonant channel is often considered in terms of successive and independent steps of photoexcitation and Auger decay. However, electron pairs emitted by the core-resonant channel also share their energy continuously to jointly conserve the energy of the complete process. By detecting the electron pairs in parallel over a wide range of energy, evidence of the core-resonant double photoemission proceeding by a coherent single-step process is most strikingly manifested by a continuum of correlated electron pairs with a sum energy characteristic of the process but for which the individual electrons have arbitrary energies and cannot meaningfully be distinguished as a photoelectron or Auger electron.

1. Introduction

The emission of two electrons from a solid surface upon the absorption of a single photon has become of much current interest due to the decisive role played by electron–electron correlation in such processes. Because of the single-particle nature of the dipole interaction, the electric field of the photon directly interacts with only a single electron. However, if the photon energy exceeds the double photoemission (DPE) threshold, two interacting electrons may be directly emitted from the valence band, sharing the photon energy in excess of that needed to eject both of them [1]. Detecting the emitted pair in coincidence with energy and momentum discrimination yields observables relevant to the electron–electron interaction in the solid [1–7]. When the energy of the incident photon exceeds the binding energy of a core-level electron, the electron is excited to the continuum above the vacuum level. A second electron may be excited to the continuum by an Auger (autoionization) transition in which the core–hole is annihilated, leaving two holes in the valence band. Auger photoelectron coincidence spectroscopy (APECS) has been

developed to study this process, motivated also by the ability to yield information not directly accessible by single-electron spectroscopy [8–16].

The emission of two electrons by core-resonant DPE proceeds through the formation of an intermediate core–hole state and is therefore often considered within a two-step model, whereby the Auger transition is treated independently from the photoemission process. Such an approximation is valid if no additional excitations occur upon creation of the core–hole intermediate state and its lifetime is sufficiently long to prevent any final-state interactions in the continuum [14, 15]. Then the photoelectron energy alone depends on the photon energy, the core–hole state can be described as a well-defined real state and the Auger electron should have energy given independently by the difference in total energy between the core–hole state and the final two-hole state. Due to the finite lifetime of the core–hole, the photoelectron energy is uncertain within its lifetime broadened width. However, when the photoelectron is detected in coincidence with the Auger electron, the uncertainty in the sum of the kinetic energy of the two electrons is due only to the lifetime broadening of the final two-hole valence state. As the

lifetime of this two-hole state is smaller than that of the core-hole state, the photoemission spectrum may be measured with energy resolution not limited by the natural linewidth [8]. This was demonstrated by measurement of the $M_{2,3}$ photoemission lines in coincidence with the $M_{2,3}$ -VV Auger line from Cu(001) with an energy resolution smaller than the lifetime broadening of the $M_{2,3}$ core-hole state [10, 12]. The coincident photoelectron lines were narrowed compared to those of the total (noncoincidence) photoelectron spectrum and the energy position of their maximum showed, within the lifetime-broadened photoelectron linewidth, linear dispersion with the energy of the detected Auger electron [10]. This behaviour shows that the Auger process is not independent of photoemission and was interpreted as evidence of the inadequacy of the two-step description of photoexcitation and decay [10, 12, 17].

Earlier observations of dynamical screening effects had already led to the understanding that adequate interpretation of APECS must go beyond the independent-particle approximation and describe photoemission and Auger decay as a coherent single-step process [14, 15]. In such descriptions the core-hole may be described by virtual intermediate states spanning all excited single-electron states including the continuum. The Coulomb operator responsible for the Auger transition acts on the complete system involving both final electrons. The complete process can thus be considered a resonance in the double-photoionization continuum [17], which is particularly suitable in the present context where we also consider direct DPE processes. A complete description of both processes must account for the initial-state electron correlation and interaction of the final-state correlated wavefunction of the emitted electron pair with the crystal lattice. [1, 17, 18].

The angular correlation between correlated electron pairs emitted by core-resonant double photoemission has recently been explored in detail [12, 18]. To extend an understanding of energy sharing between the electrons of correlated pairs by direct and core-resonant DPE, electrons pairs must be detected within a large energy window without selectively constraining the energy of either electron. Core-level photoemission and Auger emission can be observed in parallel by an appropriate choice of photon energy. By applying time coincidence techniques, we can simultaneously identify within this range correlated electron pairs emitted by direct or core-resonant double photoemission. We report here the first observation of direct and core-resonant double photoemission measured simultaneously in an energy area of almost $30 \text{ eV} \times 30 \text{ eV}$. In the present paper we focus on the experimental observation that electron pairs emitted by double photoemission resonant with core excitation share the total sum of their energy continuously without their individual energies being conserved during successive steps of photoexcitation and decay or constrained to the energy with which they are observed in single-electron spectroscopy.

2. Experimental details

A new two-electron coincidence spectrometer for surfaces was implemented by combining two hemispherical energy analysers (Scienta R4000, Sweden) with wide-angle transfer

lenses. The analysers were modified by the installation of two-dimensional detectors (microchannel plates (MCP) and resistive anodes) and the lenses are operated in customized modes optimized for the requirements of high transmission with large pass energy, low mean kinetic energy and small temporal dispersion. Angular dispersion characteristics are compromised to achieve these requirements and only energy information was recorded. Constant energy resolution can be preserved independently of the electron kinetic energy, which allows DPE experiments to be extended to photon energies previously inaccessible with time-of-flight spectrometers which presently cannot achieve comparable energy resolution beyond energies $\geq 50 \text{ eV}$ [2, 6].

The spectrometer was installed at the UE56/2-PGM-2 beamline at the BESSY II storage ring [19]. Figure 1 schematically illustrates the geometry of the experiment. Linearly polarized radiation of energy 125 eV was incident upon a Cu(001) surface at a grazing angle of 10° . Electrons emitted within the solid angle of collection of the lenses are transported to hemispherical analysers that energetically disperse the electrons onto the detectors. The optical axes of the lenses define the scattering plane and are separated by 90° with one axis in the plane of the storage ring and the other perpendicular to it. The sample was oriented such that the mean take-off angles for the horizontal and vertical analyser with respect to the surface normal were 15° and 75° , respectively.

Each analyser was operated in a mode that allowed the collection of electrons within an angular range of $\approx 30^\circ$ within the xy plane (figure 1) and, simultaneously, within a 30 eV energy range centred at 50 eV. The energy range recorded in parallel by each analyser is partitioned respectively into discrete values E_1 and E_2 for the vertical and horizontal analysers in order to represent two-dimensional (2D) electron pair energy distributions. The total energy resolution for each analyser was $\approx 0.8 \text{ eV}$. Consequently the total energy resolution for electron pairs was $\approx 1.1 \text{ eV}$. All kinetic energies were measured with respect to the vacuum level of the Cu(001) surface.

The Cu(001) single crystal was chosen as a target due to its well-known electronic structure. It was cleaned by the standard procedures of Ar^+ sputtering and annealing at 750 K before initial measurements and every 12 h thereafter. The base pressure of the chamber was $5 \times 10^{-11} \text{ mbar}$. The sample was at room temperature during the measurements.

A timing coincidence logic unit was used to determine when an electron was detected at each of the two detectors within a relatively large time range of 150 ns and to provide a timing signal relative to which the arrival time of each electron t_1 and t_2 was measured. For each such event, the energy of the two electrons and their arrival times were recorded in list mode (E_1, E_2, t_1, t_2). The distribution of the differences between the arrival times of the two electrons, $\Delta t = t_1 - t_2$, was then analysed to distinguish *true* coincidences of two correlated electrons instantaneously emitted after the absorption of a single photon from *random* coincidences of two unrelated electrons arriving at each of the detectors due, typically, to the absorption of two photons within the 150 ns time window. True

coincidences are characterized by having a Δt value within a narrow range t_c determined by the temporal resolution of the apparatus which is dominated by the energy and emission-angle-dependent temporal dispersion of the electron optics. The Δt value for fortuitously time-coincident but uncorrelated electrons is randomly distributed across the 150 ns time window. By well-established methods [20, 21] the energy-dependent background of random coincidences can therefore be subtracted from the energy distribution of true correlated pairs. The ratio of the rates of true and random coincidences was maintained above one for all spectral features of interest by reducing the photon flux at the sample by a series of apertures.

3. Experimental results and discussion

Figure 2(a) shows a histogram of arrival time differences Δt for all detected pairs from a Cu(001) surface upon excitation with linearly polarized photons of energy 125 eV. The area of the prominent peak (shaded) at $\Delta t = 0$ ns that lies above the flat background is a measure of the total number of true coincidences. Its width t_c is consistent with an estimation of the temporal resolution by simulating the dominant contribution of time dispersion through the electron optics. The number of correlated events (true coincidences) N_t is found from the total number of counts within a region of width t_c centred on the peak minus the number of random coincidence events in the same area which is estimated from the average intensity away from the peak.

The 2D energy distribution of correlated electron pairs (true coincidences) detected from the Cu(001) surface upon excitation with 125 eV photons is presented in figure 2(b). This data is obtained by determining the number of true coincidences at each locus (E_1, E_2) by the method described above. Several distinctive spectral features appear that have not previously been observed together in a single spectrum from a solid surface. The highest energy structure is related to the onset of direct DPE. Below that there are three regions of interest labelled as A, B and C which are situated around $(E_1, E_2) = (56 \text{ eV}, 46 \text{ eV})$, $(46 \text{ eV}, 56 \text{ eV})$ and $(46 \text{ eV}, 58 \text{ eV})$, respectively. These regions correspond to the nominal energy of 3p photoelectrons and $M_{2,3}-M_{45}M_{45}$ Auger electron pairs, i.e. the process studied by APECS. Their structure in and between these regions is considered in more detail below. The difference in the sum energy of the detected pairs emitted by these processes will be discussed elsewhere.

We first turn our attention to the onset of the DPE process. In the DPE process, a photon of energy $h\nu = 125 \text{ eV}$ excites the system and two unbound electrons may be detected with kinetic energy E_1 and E_2 after they have overcome the vacuum barrier given by the work function ϕ of the sample. By energy conservation, the electron pair sum energy is given by

$$E_{\text{sum}} = E_1 + E_2 = h\nu - (E_{b_1} + E_{b_2}) - 2\phi \quad (1)$$

where E_{b_1} and E_{b_2} are the electrons' bound-state energies as measured from the Fermi level E_F . The work function ϕ for the Cu(001) surface is 4.63 eV [22]. If both detected electrons were ejected from the Fermi level ($E_{b_1} + E_{b_2} = E_F$) their

sum energy would be 115.7 eV. However, it is known that the density of states at E_F , due to sp states, is small compared to the density of 3d states approximately 2 eV below E_F . In the 2D pair energy distribution (figure 2(b)) the onset of direct DPE can be easily recognized as a continuous line at a pair sum energy $E_A = E_{\text{sum}} \approx 112 \text{ eV}$ below which the coincident electron pair intensity increases. The continuous distribution of pair intensity at the onset is characteristic of the pair conserving the sum of their energy but sharing it continuously. The pair sum energy at the DPE onset corresponds to $E_{b_1} = E_{b_2} = 1.9 \text{ eV}$, which is consistent with the initial bound state of the emitted electrons being located at the top of the d-band. Thus the onset of the DPE process is dominated by the bulk d-band electrons of the Cu(001) surface.

For a photon energy $h\nu = 125 \text{ eV}$, 3p photoelectrons and $M_{23}-M_{45}M_{45}$ Auger electrons can be distinguished on the basis of the difference in their nominal energy. Accordingly, the intensity at region A would be attributed to 3p photoelectrons detected by the vertical (E_1) analyser and Auger electrons by the horizontal (E_2) analyser; similarly, intensity at B would be due to 3p photoelectrons detected by the horizontal analyser and Auger electrons by the vertical analyser. By applying the constraints to the data that E_1 (E_2) lies in the range of either $2p_{1/2}$ or $2p_{3/2}$ photoemission, a line profile along E_2 (E_1) reveals the coincident spectrum containing only the $M_2-M_{45}M_{45}$ or $M_3-M_{45}M_{45}$ ($M_3-M_{45}M_{45}$ or $M_2-M_{45}M_{45}$) Auger component, respectively. The results of this process (not shown) are equivalent to scanning over the Auger spectrum with one analyser while keeping the other fixed at a particular kinetic energy and are in general agreement with the recent work of Gotter *et al* [12]. Structure in the regions labelled A, B and C can be attributed to the spin-orbit splitting ($\approx 2.5 \text{ eV}$) of the M_{23} level, which also manifests in the corresponding $M_2-M_{45}M_{45}$ and $M_3-M_{45}M_{45}$ Auger energy and the multiplet structure of the Auger final state. The Coster-Kronig preceded $M_3M_{45}-M_3M_{45}M_{45}$ Auger process can be expected to make only a small contribution overlapping that of the $M_3-M_{45}M_{45}$ process [10]. Most clearly seen, the 1G and 3F multiplet components associated with the configuration of the two-hole final state that dominates the Auger spectrum are separated by $\approx 3 \text{ eV}$ [12]. The intensity at regions A and C in figure 2(b) can be attributed, respectively, to transitions resulting in 1G and 3F two-hole final states. We briefly note here that asymmetry about the line $E_1 - E_2$, including the absence of an intense feature corresponding to C at $(E_1, E_2) = (46 \text{ eV}, 58 \text{ eV})$, is related to the asymmetric scattering geometry which influences the relative contribution of the final multiplet components by constraining the emission direction of both electrons as reported by Gotter *et al* [12].

The structures in the regions labelled A, B and C have a diagonally oriented structure which is characteristic of a pair of electrons sharing the sum of their energy. Energy sharing between Auger and photoelectrons has previously been inferred from the shifts in the Cu 3p photoelectron line in coincidence with Auger electrons from several discrete energy ranges within the Auger envelope [10, 12]. The linear relationship between the energy of the correlated electrons is clearly evident in the 2D representation of the pair energy

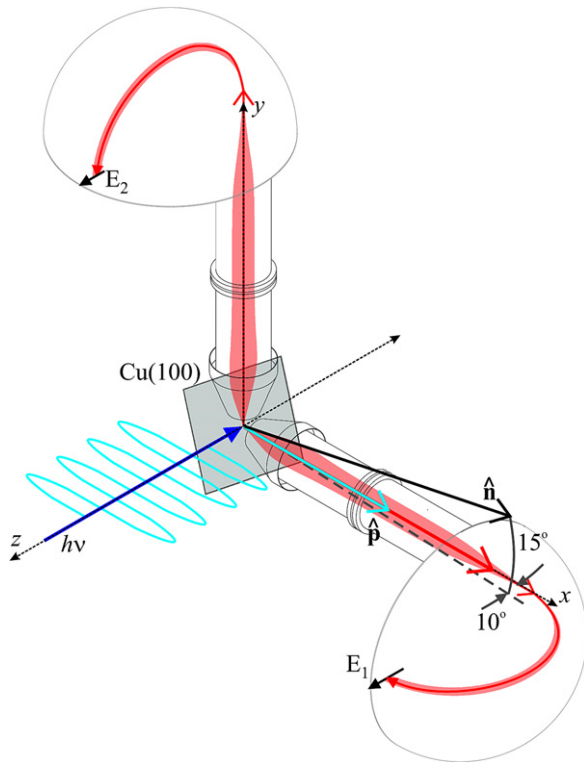


Figure 1. The schematic view of experimental set-up showing in outline the two analysers and their orientation. The light was incident on the Cu(001) crystal surface at a grazing incidence of 9.6° . The axis of the analyser transfer lenses lies in a plane perpendicular to the incident light and at an angle of 90° to each other. The energy dispersing directions are marked E_1 and E_2 , respectively. \hat{n} is the surface normal while \hat{p} gives the direction of light polarization.

distribution. A striking aspect revealed by the present work is the continuous diagonal structure of constant sum energy that connects regions A and B, extending even to where $E_1 = E_2$, where the former distinction made between Auger electron and photoelectron becomes completely meaningless.

In previous APECS experiments the energy of one fixed analyser scanned [8–13], which imposes a constraint on the uncertainty of one electron and consequently on the other electron of the correlated pair. By detecting correlated pairs over a wide energy range without imposing any restriction on the energy of either electron we reveal that the energy of both electrons is not strictly limited to the lifetime-broadened lines that are observed when each electron is detected individually by single-electron (noncoincidence) spectroscopy. This provides dramatic evidence for the inadequacy of a two-step description of the process in terms of photoexcitation and Auger decay and highlights the significance of correlation between the emitted electron pair.

We have confirmed that the continuous line between regions A and B is not an artefact by decreasing the photon energy by 5 eV to 120 eV. For this case the energy differences between the photoelectrons and Auger electrons increase and result in a larger separation between the maxima in the sharing curve. A continuous line of pair intensity still extends through $E_1 = E_2$. It is worth noting also that $h\nu = 120$ eV is below the 3s level threshold.

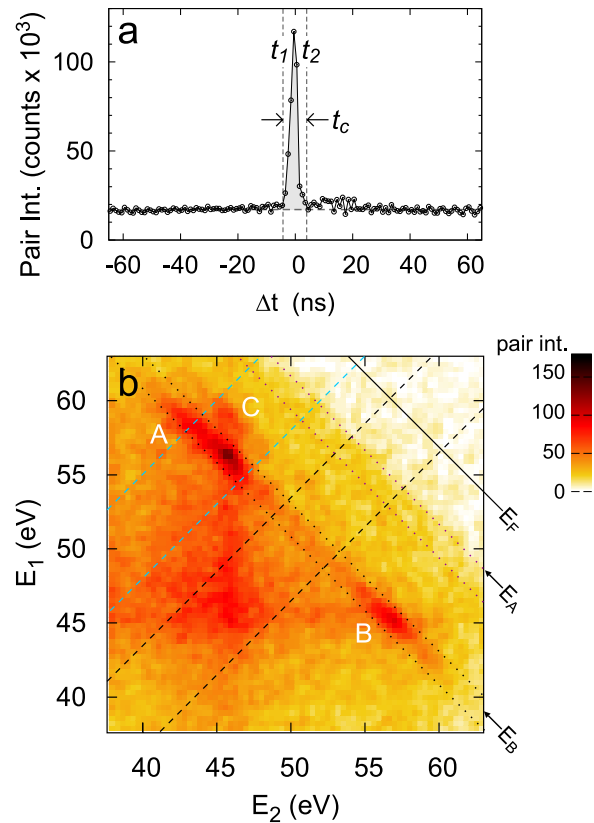


Figure 2. Experimental data from a Cu(001) surface excited by linearly polarized 125 eV photons. In panel (a) the coincident pair intensity is displayed as a function of Δt for all detected pairs. The shaded region represents the total number of true coincidences (correlated pairs) which fall within an interval $t_1 \leq \Delta t \leq t_2$. The contribution of random coincidences in this interval is estimated from the height of the constant background outside the interval. The energy distribution of the correlated pairs displayed in panel (b) was obtained by subtracting the distribution of random coincidences from the distribution of all events in intervals $t_1 \leq \Delta t \leq t_2$. E_F , E_A and E_B which label, respectively the Fermi level, the onset for direct DPE from the d states and the most intense part of the core-resonant DPE. Structures within the core-resonant DPE envelope are labelled A, B and C. Dashed and dotted lines indicate the boundary of areas from which the sum energy ($E_1 + E_2$) and energy sharing ($E_1 - E_2$) profiles in figure 3 are obtained. See the text for further details.

It is evident in the finite width of the line between A and B that the sum energy of the electron pair is conserved and constrained by the lifetime-broadened width of the final two-hole state. This can be examined more closely by constructing a sum energy spectrum under the constraint $E_1 - E_2 \approx 0$, i.e. the integrated pair intensity along a 5 eV wide region centred on $E_1 - E_2 = 0$ eV and bound between the dashed black lines in figure 2(b). The result is shown in figure 3(a). The sum energy spectrum across the region containing the features labelled A and B in figure 2(b) (the integrated pair intensity along $E_1 - E_2 = 11.5$ eV) is included for comparison. In both profiles the onset of d-band DPE at around 112 eV can be recognized. The peak at lower sum energy may be attributed predominantly to electron pairs emitted by the core-resonant DPE process, which result in a $^1G M_{45}M_{45}$ Auger final state. A smaller component attributable to 3F final states appears as an

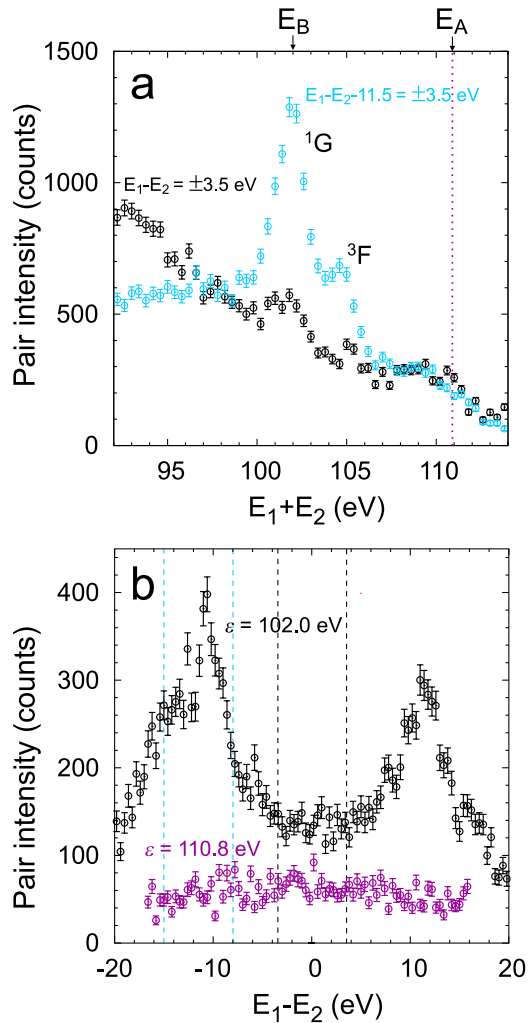


Figure 3. (a) The pair sum energy spectra of electron pairs with energy difference $E_1 - E_2 + 11.5 \text{ eV} = \pm 3.5 \text{ eV}$ (blue circles) and nearly equal energy $E_1 - E_2 = \pm 3.5 \text{ eV}$ obtained by integrating the pair intensity along the region bound by the pairs of dashed lines in figure 2(b). In both spectra both the onset of direct DPE from the d-band and DPE resonant with 3p excitation can be recognized. Lines corresponding to those in figure 2(b) are included for reference. (b) The energy sharing curves of electron pairs with sum energies of $E_1 + E_2 = \varepsilon \pm 0.9 \text{ eV}$ for $\varepsilon = 102 \text{ eV}$ (black circles) and $\varepsilon = 110.8 \text{ eV}$ (magenta circles) obtained by integrating the pair intensity along the regions bound by the pairs of dotted lines in figure 2(b). The former corresponds to electron pairs emitted by the core-resonant DPE process, resulting in a $^1G M_{45}M_{45}$ final state configuration. The latter corresponds to pairs emitted by direct DPE of electron pairs from the top of the d-band.

energy shoulder on the high energy side of the 1G component. The width of these components, taking into account the experimental resolution, can be estimated from the present data to be 1.6 eV. This is consistent with the pair sum energy being uncertain within the lifetime-broadened width of the two-hole final state.

The energy sharing distribution of correlated electron pairs can be extracted from the 2D electron pair energy distribution as the integrated intensity along a 1.3 eV wide region centred on the line $E_1 + E_2 - \varepsilon = 0$, where ε is the sum energy available to a pair for a particular process. In figure 3(b) we present a

sharing curve for $\varepsilon = 102 \text{ eV}$ that corresponds energetically to $3p_{1/2}$ and $3p_{3/2}$ photoemission and Auger transitions to $^1G M_{45}M_{45}$ final states (small overlapping contribution from other final states can be neglected). The region is shown bound by dotted black lines in figure 2(b). The sharing curve for $\varepsilon = 111 \text{ eV}$ that corresponds to direct DPE final states, included in figure 3(b), is comparatively flat. The broad peaks in the energy sharing distribution (figure 3(b)) for pairs emitted by core-resonant DPE may suggest that the energy sharing between electrons is not completely arbitrary and may be sensitive to the particular initial, intermediate and final states involved in each of the allowed transitions. Detailed analysis of the shape of the peaks in the sharing curves requires consideration of the angle-dependent contribution from each transition due to dipole and Coulomb selection rules, together with diffraction of the electron pairs within the crystal and the discrimination between the transitions imposed by the arrangement of the detectors [12]. It should be added that the origin of the intensity extending in broad bands from region A in the $-E_1$ direction and from region B in the $-E_2$ direction and overlapping around $(E_1, E_2) = (45, 45)$ is not yet completely understood. The direction of these bands, parallel to the energy axes, is characteristic of nonconservation of the sum energy of the pair due to inelastic scattering processes. The contribution of an incoherent process and its influence in the sharing curve for the electrons emitted by core-resonant DPE will be investigated in future experiments.

To explain the continuous energy sharing we consider that the system is collectively excited upon absorption of the photon into an intermediate many-body state that cannot be decomposed into products of single-particle states. The system decays to a two-hole final state by the emission of a pair of electrons in an interacting two-particle state. The emitted electrons should therefore be regarded as a single entity. There is, in principle, no constraint on the energy of each electron but they may arbitrarily share the total energy available which is determined by energy conservation of the complete process. In this regard the processes of direct and core-resonant DPE are similar. We emphasize that without Coulomb interaction neither process can occur. If the coherence of the two-particle state is broken by, for example, inelastic scattering, it will decay into single-particle states and each electron will be observed with an average energy equal to the nominal photoelectron or Auger electron energy. Similarly, the two-particle nature of the emitted electrons can only be observed when both electrons are detected and correlated in time. The spectra observed by single (noncoincidence) photoelectron or Auger electron spectroscopy may be considered to be equivalent to the pair spectrum integrated over all possible emission directions and energy of the undetected electron.

4. Conclusions

We have presented the two-particle emission spectra from a Cu(001) surface upon excitation with linearly polarized photons with sufficiently high energy to excite the 3p core level. We observe both direct DPE and core-resonant DPE in the same spectrum. The final state of both processes

contain two holes in the d-band but is distinguished on the basis of the total energy available to the pair. In the energy sharing distribution of electron pairs, the direct DPE manifests as a continuum without discrete structure. Pairs emitted by core-resonant double photoemission are also clearly shown to share their total energy continuously while jointly conserving the energy of the complete process. The energy of both electrons is not constrained to the energy they are observed to have when detected independently. These results confirm that core-resonant double photoemission must be described by a coherent single-step process in which the emitted electrons represent a correlated two-particle state. Detailed comparison of the dynamics of direct double photoemission and core-resonant double photoemission is currently being investigated for different scattering geometries and photon energies and is expected to yield further insight into the role of correlation in these processes.

Acknowledgments

We thank the BESSY II staff, particularly W Mahler and B Zada, for excellent experimental conditions at the beamline.

References

- [1] Berakdar J 1998 *Phys. Rev. B* **58** 9808
- [2] Schumann F O, Winkler C and Kirschner J 2007 *Phys. Rev. Lett.* **98** 257604
- [3] Fominykh N, Henk J, Berakdar J and Bruno P 2002 *Surf. Sci.* **507–510** 229
- [4] Fominykh N, Henk J, Berakdar J, Bruno P, Gollisch H and Feder R 2000 *Solid State Commun.* **113** 665
- [5] Fominykh N, Berakdar J, Henk J and Bruno P 2002 *Phys. Rev. Lett.* **89** 086402
- [6] Herrmann R, Samarin S, Schwabe H and Kirschner J 1998 *Phys. Rev. Lett.* **81** 2148
- [7] Gollisch H, v Schwartzberg N and Feder R 2006 *Phys. Rev. B* **74** 075407
- [8] Sawatzky G A 1988 *Treatise on Materials Science and Technology* ed C L Briant and R P Messmer (New York: Academic) pp 167–243
- [9] Haak H W, Sawatzky G A and Thomas T D 1978 *Phys. Rev. Lett.* **41** 1825
- [10] Jensen E, Bartynski R A, Hulbert S L, Johnson E D and Garrett R 1989 *Phys. Rev. Lett.* **62** 71
- [11] Stefani G, Gotter R, Ruocco A, Offi F, Pieve F D, Iacobucci S, Morgante A, Verdini A L A, Yao H and Bartynski R A 2004 *J. Electron. Relat. Phenom.* **141** 149
- [12] Gotter R, Da Pieve F, Offi F, Ruocco A, Verdini A, Yao H, Bartynski R and Stefani G 2009 *Phys. Rev. B* **79** 075108
- [13] van Riessen G A and Thurgate S M 2006 *Surf. Int. Anal.* **38** 691
- [14] Gunnarsson O and Schönhammer K 1980 *Phys. Rev. B* **22** 3710
- [15] Ohno M and Wendin G 1979 *J. Phys. B: At. Mol. Phys.* **12** 1305
- [16] Ohno M 1999 *J. Electron Spectrosc. Relat. Phenom.* **109** 109
- [17] Stefani G, Iacobucci S, Ruocco A and Gotter R 2002 *J. Electron. Relat. Phenom.* **127** 1
- [18] Da Pieve F, Sebilliau D, Di Matteo S, Gunnella R, Gotter R, Ruocco A, Stefani G and Natoli C R 2008 *Phys. Rev. B* **78** 035122
- [19] Sawhney K, Senf F, Scheer M, Schafers F, Bahrdt J, Gaupp A and Gudat W 1997 *Nucl. Instrum. Methods* **390** 395
- [20] Jensen E, Bartynski R A, Hulbert S L and Johnson E D 1992 *Rev. Sci. Instrum.* **63** 3013
- [21] Hayes P, Bennett M A, Flexman J and Williams J F 1988 *Rev. Sci. Instrum.* **59** 2445
- [22] Weinelt M 2002 *J. Phys.: Condens. Matter* **14** R1099